Contents lists available at ScienceDirect

Chemical Engineering Research and Design

journal homepage: www.elsevier.com/locate/cherd

Continuous reaction crystallization of struvite from diluted aqueous solution of phosphate(V) ions in the presence of magnesium ions excess

Anna Kozik[a], *Nina Hutnik*[a], *Krzysztof Piotrowski*[b,*], *Andrzej Matynia*[a]

[a] *Wroclaw University of Technology, Faculty of Chemistry, Wybrzeze Wyspianskiego 27, 50-370 Wrocław, Poland*
[b] *Silesian University of Technology, Department of Chemical & Process Engineering, ks. M. Strzody 7, 44-101 Gliwice, Poland*

A B S T R A C T

Continuous reaction crystallization of struvite $MgNH_4PO_4{\cdot}6H_2O$ from diluted aqueous solution containing phosphate(V) ions of concentration 0.20 wt% PO_4^{3-} was investigated experimentally. The tests were carried out in a continuous DT MSMPR type crystallizer in temperature 298 K assuming 20% excess of magnesium ions at the inlet point in respect to struvite synthesis reaction stoichiometry. Influence of pH (8.5–10) and mean residence time of suspension in a crystallizer (900–3600 s) on the product crystals size distribution, their size-homogeneity and process kinetics were identified. Crystals of mean size from ca. 19 to ca. 73 μm, of diverse size-homogeneity (CV 60–87%) were produced. Struvite particles of the largest sizes and acceptable homogeneity were produced at pH 8.5 for prolonged mean residence time 3600 s. Under these conditions struvite nucleation rate did not exceed 5.3×10^7 l/(s m^3) according to SIG MSMPR model predictions. Crystal linear growth rate within the investigated process parameter values varied from 3.62×10^{-9} to 1.68×10^{-8} m/s. Magnesium ions excess in a process environment influenced yield of continuous reaction crystallization of struvite advantageously – contrary to product crystals quality. Concentration of phosphate(V) ions in mother solution decreased from inlet 0.20 wt% to 0.9×10^{-3} – 9.2×10^{-3} wt% (9–92 mg/kg) depending on pH and mean residence time of suspension in a crystallizer, what can be regarded as a very good result of their recovering from solution.

Keywords: Struvite; Reaction crystallization; Continuous DT MSMPR crystallizer; Magnesium ions excess; Crystal size distribution; SIG MSMPR kinetic model

1. Introduction

Modern technologies of phosphate(V) ions recovery from wastewater or liquid manure are based on precipitation followed by mass crystallization of sparingly soluble phosphate(V) salt(s), usually magnesium ammonium phosphate(V) hexahydrate, $MgNH_4PO_4{\cdot}6H_2O$ (MAP, struvite) (Le Corre et al., 2009). Struvite precipitates after contacting the reagents: magnesium (e.g. magnesium chloride) and ammonium ions (e.g. ammonium chloride) with some aqueous solution containing phosphate(V) ions, contributed by proper adjustment of the resulting mixture pH (Parsons, 2001). Providing optimal process conditions for the controlled continuous reaction crystallization of struvite is a complex technological problem (Doyle and Parsons, 2004; de-Bashan and Bashan, 2004; Le Corre et al., 2009; Karabegovic et al., 2013). Final effect – crystal population of determined chemical purity and size distribution, manufactured with satisfactory yield – depends on many parameters defining environment in which struvite reaction crystallization runs (Doyle and Parsons, 2002; Matynia et al., 2006; Le Corre et al., 2007a; Hutnik et al., 2013), as well as on the crystallizer construction used (Bhuiyan et al., 2008; Le Corre et al., 2009; Mazienczuk et al., 2012). Struvite precipitates in supersaturated solutions of phosphate(V), magnesium and ammonium ions, within pH range of 7–11. Struvite solubility product pK_{sp} values from 9.40 to 13.36

* *Corresponding author*. Tel.: +48 32 237 1900; fax: +48 32 237 1461.
E-mail address: krzysztof.piotrowski@polsl.pl (K. Piotrowski).
Received 21 November 2012; Received in revised form 23 July 2013; Accepted 31 August 2013
0263-8762/$ – see front matter © 2013 The Institution of Chemical Engineers. Published by Elsevier B.V. All rights reserved.
http://dx.doi.org/10.1016/j.cherd.2013.08.032

Nomenclature

B	nucleation rate, 1/(s m^3)
d	crystallizer diameter, m
d_{dt}	draft tube diameter, m
d_m	stirrer diameter, m
G	crystal linear growth rate, m/s
h_{dt}	draft tube height, m
h_t	crystallizer total height, m
h_w	crystallizer working part's height, m
k_v	crystal volume shape factor
K_{sp}	solubility product
L	crystal characteristic size, m
L_a	crystal length, m
L_b	crystal width, m
L_c	crystal height, m
L_d	dominant (mode) crystal size, m
L_i	mean size of i-th crystal fraction, m
L_m	mean crystal size, m
L_{50}	median crystal size, m
L_{84}, L_{16}	crystal sizes corresponding to 84 and 16 wt% undersize fractions, m
m_i	mass of i-th crystal fraction, kg
M_T	solid phase concentration in a product crystal suspension, kg/m^3
$[Mg^{2+}]_{RM}$	concentration of magnesium ions in a feed, wt%
n	crystal population density, 1/(m m^3)
n_i	population density of i-th crystal fraction, 1/(m m^3)
n_0	nuclei population density, 1/(m m^3)
$[NH_4^+]_{RM}$	concentration of ammonium ions in a feed, wt%
$[PO_4^{3-}]_{ML}$	concentration of phosphate(V) ions in mother liquor, mg/kg
$[PO_4^{3-}]_{RM}$	concentration of phosphate(V) ions in a feed, wt%
T	reaction crystallization process temperature, K
$V_{crystal}$	real volume of the crystal, m^3
V_i	volume of i-th crystal fraction, m^3
V_t	total volume of the crystallizer, m^3
V_w	working volume of the crystallizer, m^3
x_i	mass fraction of crystals of mean fraction size L_i
Δc	supersaturation, mg/kg
ΔL_i	size width of i-th crystal fraction, m
ρ	crystal density, kg/m^3
τ	mean residence time of suspension in a crystallizer, s
CSD	crystal size distribution
CV	coefficient of variation of crystal size
DT	draft tube
GRD	growth rate dispersion
IWW	phosphorus fertilizers industry wastewater
MAP	magnesium ammonium phosphate(V) hexahydrate, struvite
MSMPR	mixed suspension mixed product removal crystallizer
SDG	size dependent growth
SIG	size independent growth
SWW	synthetic wastewater

are reported in literature (Doyle and Parsons, 2002; Bhuiyan et al., 2007). Most of published works about struvite nucleation and its crystals growth under supersaturation control (Kofina and Koutsoukos, 2005; Ali and Schneider, 2006) assume $pK_{sp} = 13.26$ (Ohlinger et al., 1998). For this pK_{sp} equilibrium concentration of phosphate(V) ions is 3.6 mg/kg. In reality, however, this value is unknown. It depends on many process (e.g. solution composition, component concentrations), technological (e.g. pH) and even constructional parameters (e.g. mixing and/or circulation method, mixing intensity and efficiency) (Le Corre et al., 2009). Clear-cut determination of metastable zone width and working supersaturation Δc in a real struvite reaction crystallization system is thus a complex problem (Ali and Schneider, 2006; Gadekar and Pullammanappallil, 2010). Some method for estimation of working supersaturation Δc in dynamic process conditions, for specific system of struvite reaction crystallization in the assumed crystallizer configuration was presented by Doyle and Parsons (2002). This method, however, does not provide one with the creditable data. One of the reasons is that for very fast (practically instant) ionic reaction of struvite precipitation very high supersaturation values (thus high nucleation (even homogeneous) rates) are observed. This effect is especially distinct close to both crystallizer inlet ports – of feed (initially premixed reagents) and of alkalizing solution (pH correcting agent) (Matynia et al., 2006; Le Corre et al., 2007a). Local supersaturation, of value many time higher than the volume – averaged working supersaturation, is a main factor determining nuclei population density, thus indirectly final product's CSD (*Crystal Size Distribution*) (Söhnel and Garside, 1992). In a continuous crystallizer, for constant in time feed composition and other work parameters (mixing intensity), working supersaturation can be indirectly represented by unequivocally correlated mean residence time of suspension, τ (Mullin, 1993). Possibly precise determination of effect of process decisive parameters (feed composition, pH, τ, etc.) on this process results (CSD, kinetic parameter values, etc.) is thus possible (Mersmann, 1995).

One of fundamental technological parameters is pH. With pH increase struvite solubility decreases (minimal K_{sp} value corresponds to pH 10.3 (Ohlinger et al., 1998) or 10.7 (Snoeyink and Jenkins, 1980)) and its precipitating potential grows (Parsons, 2001). Also induction time, necessary for initiation of batch nucleation process, shortens (Bouropoulos and Koutsoukos, 2000; Kofina and Koutsoukos, 2005; Le Corre et al., 2007b). Final result of struvite reaction crystallization depends also on process operation mode (batch, semi-batch or continuous) and crystallizer construction (e.g. fluidal bed, with internal suspension circulation), intensity of mixing and/or circulation of solution or suspension, temperature, chemical composition of wastewater, reagent ratios, etc. (Ali and Schneider, 2006; Bhuiyan et al., 2008; Matynia et al., 2006; Le Corre et al., 2007a; Marti et al., 2010; Mazienczuk et al., 2012; Karabegovic et al., 2013). Impurities present in wastewaters, mainly metal ions, but also sulphates(VI), nitrates(V) and carbonates influence struvite nucleation and its crystals growth, crystal shape and agglomeration, as well as chemical composition of final product (co-precipitated sparingly soluble hydroxides or phosphates(V) of selected metal impurities) (Hutnik et al., 2013). Catalyzing or inhibiting effects of individual ionic impurities (Hutnik et al., 2011a) depend on crystallization mode, crystallizer type and its work parameters (e.g. recovery of struvite in calcium ions presence in batch crystallizer (Le

Corre et al., 2005) and in continuous crystallizer (Hutnik et al., 2011b)).

Complex influence of various factors and observed feedbacks require possibly fully controlled conditions for struvite production from wastewaters (Le Corre et al., 2009). Recovered solid product should be of good quality. Struvite crystals should be prismatic or needle, homogeneous and of large size. Product should not contain too large amount of impurities co-precipitated from wastewater (Hutnik et al., 2013). This product can be practically utilized e.g. as mineral fertilizer (NPMg) in agriculture (de-Bashan and Bashan, 2004; Latifian et al., 2012).

Not many works concerning typical aspects of continuous mass crystallization of struvite (after precipitation) were published (Matynia et al., 2006; Hutnik et al., 2013). Usually more attention is paid on first stage of phosphates(V) recovery – struvite precipitation, neglecting specific requirements of the second stage of this process – mass crystallization (Le Corre et al., 2009; Marti et al., 2010).

Experimental research results concerning continuous reaction crystallization of struvite from synthetic wastewater, containing 0.20 wt% PO_4^{3-} ions are presented and discussed. Tests were carried out in laboratory DT MSMPR (*Draft Tube, Mixed Suspension Mixed Product Removal*) type crystallizer with internal circulation of suspension driven by propeller stirrer (Mullin, 1993). Crystallizer was provided with a feed (synthetic wastewater with appropriate substrates premixed) of assumed molar ratio PO_4^{3-}:Mg^{2+}:NH_4^+ set as 1:1.2:1. Process ran in constant temperature 298 K. Influence of pH (8.5–10) and mean residence time of suspension in a crystallizer (τ 900–3600 s) on the product quality was identified. From the product CSDs nucleation rates and linear growth rates were estimated. Simplified model of mass crystallization kinetics in a continuous MSMPR crystallizer – SIG (*Size Independent Growth*) model was adopted for kinetic data estimation (Mullin, 1993; Randolph and Larson, 1988).

2. Materials and methods

2.1. Setup and procedure

Schematic diagram and photos of experimental plant are presented in Fig. 1. It is fully automated research plant *Bioengineering RALF Plus Solo*. Steering, control and acquisition of measurement data were carried out with the use of PC computer driven by *BioScadaLab* software. Investigated continuous struvite reaction crystallization process was carried out in a laboratory DT MSMPR type crystallizer of working volume V_w 0.6 dm^3 (total volume V_t 1.3 dm^3). Crystallizer, made of glass, was equipped with heating/cooling coil for stabilization of the required process temperature. Providing the crystallizer interior with compressed air for eventual stripping of absorbed CO_2 or oxidation of organic/inorganic substances present in real wastewaters is also possible. Crystallizer diameter was d 100 mm, its working part's height h_w 90 mm while total height h_t 200 mm. In the crystallizer's central axis the circulation profile element (DT, d_{dt} 52 mm, h_{dt} 50 mm) was fixed, inside which four-paddle propeller stirrer of diameter d_m 48 mm operated. Stirrer speed, process temperature, inlet compressed air stream, inlet streams of feed and alkalizing solution, as well as outlet stream of product crystal suspension from the crystallizer were rigorously controlled and regulated by computer.

Crystallizer was continuously provided with a feed – aqueous solution of ammonium dihydroxyphosphate(V) $NH_4H_2PO_4$ and magnesium chloride $MgCl_2$. Solution was prepared in external mixed vessel using crystalline $NH_4H_2PO_4$, crystalline $MgCl_2{\cdot}6H_2O$ (p.a., POCh Gliwice, Poland) and deionized water (Barnstead-NANOpure DIamond). Feed solution was introduced into circulation profile (stirrer speed: 4.0 1/s; suspension movement – downward). Between crystallizer body and circulation profile (DT) (suspension movement – upward) aqueous solution of sodium hydroxide of concentration 3 wt% NaOH was dosed providing the assumed pH of struvite reaction crystallization environment. The research ran in temperature 298 (±0.2) K assuming pH 8.5, 9 or 10 (±0.1) and mean residence time of suspension in a crystallizer τ 900, 1800 or 3600 s (±20 s). Reagent concentrations in a feed were: $[PO_4^{3-}]_{RM}$ = 0.20 wt%, $[Mg^{2+}]_{RM}$ = 0.0614 wt% and $[NH_4^+]_{RM}$ = 0.0380 wt%, providing their molar ratio 1:1.2:1. Compressed air stream (100 Ndm^3/h, pressure ca. 2.5 bar) was provided into the crystallizer below stirrer paddles operating space. Since the synthetic wastewater contained only reagent and chloride ions, air barbotage contributed mixing intensity within struvite crystal suspension only. In case of feeding the crystallizer with real wastewater (containing various impurities, CO_2) one can directly compare the research results since identical hydrodynamic conditions are provided (e.g. Kozik et al., 2013). After stabilization in a crystallizer the assumed parameter values, process in a steady state ran through the next 5τ. After this time there were determined – with appropriate analytical methods – solid phase concentration in a product crystal suspension (M_T), chemical composition of mother liquor and solid phase (atomic absorption spectrometer iCE 3000, spectrophotometer UV–VIS Evolution 300), size distribution of struvite crystals (solid particle analyzer Beckman Coulter LS 13-320) and their shape (computer aided analysis of images provided by scanning electron microscope JEOL JSM 5800LV). Accuracy of measurement data concerning complex continuous struvite reaction crystallization process in a computer-controlled laboratory plant was estimated to be ca. 10%.

Mass-basis $m_i(L)$ (or volume-basis, $V_i(L)$) product CSDs were determined with the standard procedures of solid particle analyzer Beckman Coulter LS 13-320. Corresponding population density values, n_i, were then calculated according to Eq. (1) (Mullin, 1993):

$$n_i = \frac{m_i}{k_v \rho L_i^3 \Delta L_i V_w} = \frac{V_i}{k_v L_i^3 \Delta L_i V_w} \quad (1)$$

Volume shape factor k_v ($=V_{crystal}/L^3$) is not a constant value for all struvite crystals in a product population. Struvite crystals during growth do not maintain full geometrical similarity thus their final shape depends also on crystallization process parameters (see Section 3.2). For the calculation of population densities n_i corresponding to each product and to each crystal fraction ΔL_i within these products, k_v = 1 was assumed for simplification. This assumption does not influence linear crystal growth rate G calculated from Eq. (2) representing the most simplified SIG MSMPR kinetic model (Mersmann, 1995). Nucleation rate B (Eq. (3)) is, however, 1/k_v-time lower.

2.2. Kinetic model – size independent growth (SIG)

Experimental data were interpreted with the kinetic model of continuous MSMPR crystallizer (Mullin, 1993; Randolph and

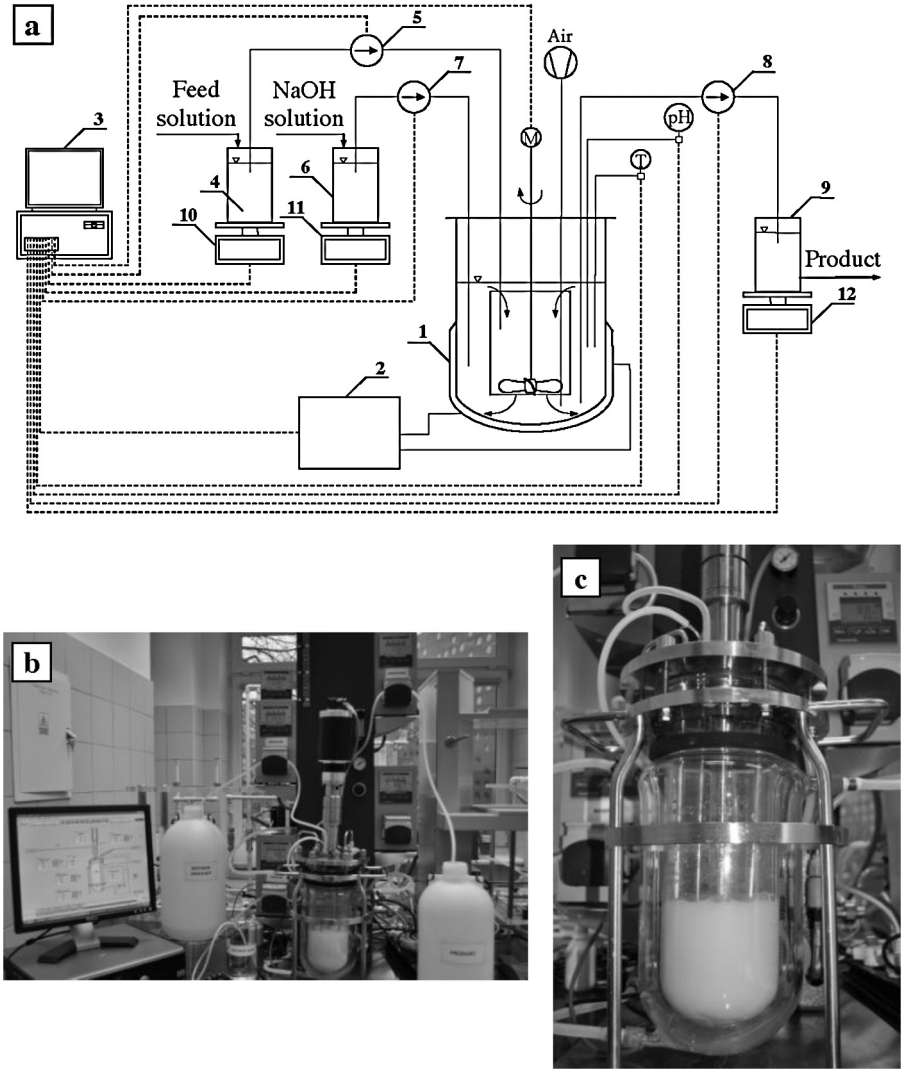

Fig. 1 – Schematic diagram of the experimental plant (a). 1 – DT MSMPR type crystallizer with internal circulation of suspension, 2 – thermostat, 3 – PC computer, 4 – reservoir of a feed: aqueous solution of $MgCl_2$ and $NH_4H_2PO_4$, 5 – feed proportioner (pump), 6 – alkalinity agent tank: aqueous solution of NaOH, 7 – proportioner (pump) of NaOH solution, 8 – receiver (pump) of product crystal suspension from the crystallizer tank, 9 – storage tank of a product crystal suspension, 10, 11, 12 – electronic balances, Air – compressed air delivery system, M – stirrer speed control/adjustment, pH – alkaline/acid reaction control/adjustment, T – temperature control/adjustment. Photos: (b) general view, (c) continuous DT MSMPR crystallizer unit with internal circulation of suspension.

Table 1 – Experimental results concerning continuous struvite reaction crystallization process in a DT MSMPR crystallizer. Reaction crystallization process temperature: 298 K. Molar proportions of reagent ions in a feed: $[PO_4^{3-}]_{RM}$:$[Mg^{2+}]_{RM}$:$[NH_4^+]_{RM}$ = 1:1.2:1.

No.	Process parameters		Crystal population characteristics				Mother liquor $[PO_4^{3-}]_{ML}$(mg/kg)
	pH	τ (s)	L_m(μm)	L_{50}(μm)	L_d(μm)	CV (%)	
1	8.5	900	32.9	23.9	28.7	82.3	92
2	9	900	26.9	16.1	21.7	85.6	25
3	10	900	18.8	12.0	14.3	86.4	21
4	8.5	1800	51.7	42.8	44.7	74.7	65
5	9	1800	37.3	25.4	34.6	82.1	12
6	10	1800	26.3	20.1	21.5	87.4	10
7	8.5	3600	72.8	65.2	66.9	59.8	40
8	9	3600	48.5	42.4	44.6	64.6	18
9	10	3600	40.1	34.4	38.0	72.3	9

Concentrations of reagent ions at a feed point: 0.20 wt% of PO_4^{3-}, 0.0614 wt% of Mg^{2+}, 0.0380 wt% of NH_4^+. Average crystal concentration in suspension: $M_T = 4.9 \pm 0.1$ kg of struvite/m^3 of suspension. $L_m = \Sigma x_i L_i$, where x_i – mass fraction of crystals of mean fraction size L_i; L_{50} – median crystal size for 50 wt% undersize fraction; L_d – crystal mode size; $CV = 100(L_{84} - L_{16})/(2L_{50})$, where L_{84}, L_{16}, L_{50} – crystal sizes corresponding to 84, 16 and 50 wt% undersize fractions.

Larson, 1988), based on the following, fundamental theoretical assumptions:

- mass crystallization process in a steady state runs in ideally mixed crystal suspension,
- aggregation, agglomeration, attrition, breakage and similar partial phenomena within the examined solid phase are not observed,
- crystals are geometrically similar (constant volume shape factor k_v); their diversity can be thus unequivocally expressed by one characteristic size L only,
- zero-size nuclei can appear only,
- non-classified, fully representative to the bulk magma population is continuously removing from the crystallizer, which size distribution results only from intrinsic kinetic feedbacks between nucleation and crystal phase growth, supplemented by diversified residence times of individual particles in the apparatus space,
- linear crystal growth rate is size-independent, SIG kinetic model ($G(L) = G = \text{const.}$ for the average supersaturation in a process system).Under these assumptions crystal population balance equation can be rearranged into the following final form, Eq. (2) (Randolph and Larson, 1988):

$$n(L) = n_0 \exp\left(-\frac{L}{G\tau}\right) \quad (2)$$

Fitting the experimental population density distribution $n(L)$ data with Eq. (2) makes estimation of the fundamental kinetic parameter values of mass (reaction) crystallization process in ideal MSMPR crystallizer configuration – B and G – possible. Graphical representation of rearranged Eq. (2) – $\ln n(L)$ – is in this case straight line, which intersection with y-axis for $L = 0$ represents $\ln n_0$ while its slope $-1/(G\tau)$. Thus, for the known – and precisely determined – slope and mean residence time of crystal suspension in a working volume of the apparatus, τ, crystal linear growth rate G can be determined directly. Knowing G and nuclei population density n_0 nucleation rate B can be calculated with Eq. (3):

$$B = n_0 G. \quad (3)$$

3. Results and discussion

3.1. Crystal size distribution

Properly shaped struvite crystals which mean size L_m varied from 18.8 up to 72.8 μm were produced, depending on the combination of process parameter values (pH–τ). Statistical parameter values of these CSDs are presented in Table 1. From the table it results, that increase in pH of mother liquor in a crystallizer did not favour production of homogeneous struvite crystals of large sizes. Increase in pH from 8.5 to 10 resulted in decrease of mean crystal size L_m from 32.9 to 18.8 μm (by ca. 43%) and from 72.8 to 40.1 μm (by ca. 45%) for τ 900 and 3600 s, appropriately. Under these conditions the CV coefficient increased from 82.3% to 86.4% and from 59.8% to 72.3%. Crystals produced at pH 10 characterized thus not only by the smallest mean particle sizes, but demonstrated also higher size-scatter.

Elongation of mean residence time of suspension in a crystallizer caused, however, increase in product crystal sizes, even more than 2-time. Struvite crystals reached mean size L_m as high as 72.8 μm for mean residence time τ 3600 s and pH

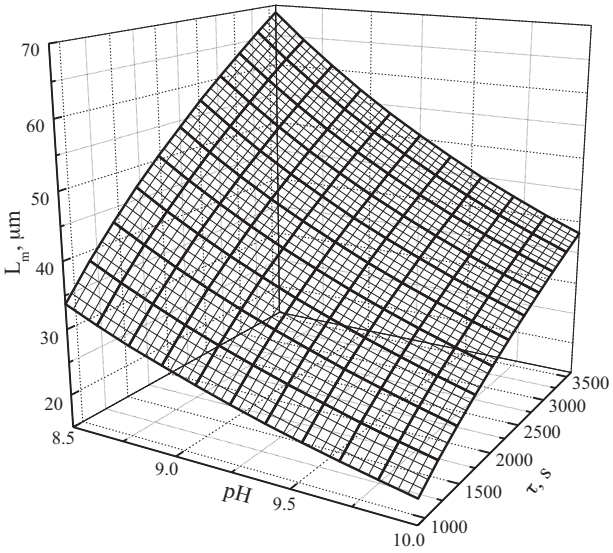

Fig. 2 – Effect of pH and mean residence time of suspension τ in a continuous DT MSMPR crystallizer on mean product crystal size, L_m (Eq. (4)).

8.5 (Table 1). With elongation of mean residence time average supersaturation in solution decreases, what results in, among others, decrease of crystals linear growth rate (see Table 2). In solution of lower average supersaturation struvite crystals grew slower, however more stable. Longer contact time of crystal phase with the supersaturated mother liquor influenced also final CSD advantageously. Homogeneity within product population increased clearly. For pH = 8.5 the CV coefficient decreased from 82.3% to 59.8% (by ca. 27%), in spite of more intense co-running processes of crystal attrition and breakage with longer residence time in a mixed and circulated suspension.

Simultaneous influence of pH in 8.5–10 range and mean residence time of suspension in a crystallizer $900 < \tau < 3600$ s on mean size of struvite crystals, L_m (in μm) can be presented in a form of empirical correlation, Eq. (4):

$$L_m = 2.45 \times 10^3 \quad \mathrm{pH}^{-3.64}\tau^{0.515} \quad (4)$$

with correlation coefficient $R^2 = 0.975$ and mean relative error ±6.0%. Graphical projection of Eq. (4) is presented in Fig. 2.

Eq. (4) correlates influence of the decisive technological parameters of struvite reaction crystallization process (pH, τ) in a continuous DT MSMPR crystallizer on mean product crystal size, L_m for the assumed feed composition, internal crystallizer geometry and determined intensity of mixing and circulation of suspension in a crystallizer (Franke and Mersmann, 1995; Penicot et al., 1998). Empirical Eq. (4) is not of general character (Söhnel and Garside, 1992). It represents $L_m = f(\mathrm{pH}, \tau)$ relation valid for the investigated continuous DT MSMPR crystallizer configuration only.

Under stoichiometric conditions ($[PO_4^{3-}]_{RM}$:$[Mg^{2+}]_{RM}$:$[NH_4^+]_{RM}$ = 1:1:1) from the same DT MSMPR crystallizer and for identical process parameter values struvite crystals of distinctly larger sizes were produced (Kozik and Matynia, 2012). Their mean size was higher by ca. 45% on average. For example, for pH 8.5 and τ 3600 s products of mean crystal size 110.2 μm (Kozik and Matynia, 2012) (see Fig. 4d) and 72.8 μm (No. 7 in Table 1, see Fig. 4b) were removed from the crystallizer, for the strict reagents stoichiometry and at 20% excess of magnesium ions in a feed, respectively. Main

Table 2 – Nucleation rate B and crystal linear growth rate G estimated for struvite reaction crystallization process in a continuous DT MSMPR crystallizer. Kinetic parameter values calculated with SIG MSMPR model. Process conditions – see Table 1.

No.[a]	Process kinetic parameters (SIG MSMPR model)				SWW[c]		IWW[d]	
	$n(L)$[b] for $L>50\,\mu m$	R^2 (for linear segment)	G (m/s)	B 1/(m^3 s)	G (m/s)	B 1/(m^3 s)	G (m/s)	B 1/(m^3 s)
1	$n=2.262\times10^{15}\exp(-6.598\times10^{4}L)$	0.987	1.68×10^{-8}	3.9×10^{7}	1.81×10^{-8}	5.0×10^{7}		
2	$n=3.024\times10^{15}\exp(-6.781\times10^{4}L)$	0.986	1.64×10^{-8}	4.9×10^{7}	1.72×10^{-8}	5.1×10^{7}	1.43×10^{-8}	3.6×10^{8}
3	$n=3.305\times10^{16}\exp(-1.165\times10^{5}L)$	0.976	9.54×10^{-9}	3.1×10^{8}	1.38×10^{-8}	2.1×10^{8}		
4	$n=1.792\times10^{15}\exp(-5.074\times10^{4}L)$	0.988	1.09×10^{-8}	2.0×10^{7}	1.15×10^{-8}	1.2×10^{7}		
5	$n=5.233\times10^{15}\exp(-7.195\times10^{4}L)$	0.999	7.72×10^{-9}	4.0×10^{7}	1.12×10^{-8}	2.0×10^{7}		
6	$n=1.462\times10^{16}\exp(-7.992\times10^{4}L)$	0.971	6.95×10^{-9}	1.0×10^{8}	1.02×10^{-8}	9.6×10^{7}		
7	$n=8.727\times10^{15}\exp(-4.558\times10^{4}L)$	0.987	6.09×10^{-9}	5.3×10^{7}	8.93×10^{-9}	1.8×10^{7}		
8	$n=1.468\times10^{16}\exp(-5.155\times10^{4}L)$	0.987	5.39×10^{-9}	8.1×10^{7}	5.91×10^{-9}	5.8×10^{7}	4.27×10^{-9}	9.0×10^{7}
9	$n=4.841\times10^{16}\exp(-7.666\times10^{4}L)$	0.989	3.62×10^{-9}	1.7×10^{8}	4.96×10^{-9}	9.0×10^{7}		

[a] See Table 1 for details.
[b] For $k_v=1$.
[c] Synthetic wastewater, stoichiometric conditions (Kozik and Matynia, 2012).
[d] Phosphorus fertilizers industry wastewater, magnesium ions excess (Hutnik et al., 2013).

reason for the observed difference is higher supersaturation of magnesium ions at the crystallizer inlet point, resulting from their excess in a feed. Higher supersaturation results in increase in struvite nuclei population density n_0 as a result of higher nucleation rate B. In result the L_m values of struvite product crystals decreased. Magnesium ions excess did not cause, however, significant changes in homogeneity of product population. Maximal difference in coefficient of crystal size variation CV in both compared test series did not exceed ±3% on average (compare (Kozik and Matynia, 2012) and Table 1). In case of real wastewater from phosphorus mineral fertilizers industry containing phosphate(V) ions of concentration 0.445 wt% and impurities (aluminium, calcium, copper, iron, potassium, titanium, zinc, silicate, fluoride, sulfate(VI) ions) one obtained in a continuous DT MSMPR crystallizer product crystals of mean size L_m 36.8 μm and CV 74.7% (pH 9, τ 3600 s, 20% excess of magnesium ions) (Hutnik et al., 2013). These were thus crystals of smaller sizes and of lower homogeneity compared to struvite produced from pure aqueous solution of PO_4^{3-}, Mg^{2+} and NH_4^+ ions (test No. 8 in Table 1). Net effect of individual impurities (Hutnik et al., 2011a) present in real wastewater on struvite CSD turned out to be disadvantageous.

In Fig. 3 there are presented exemplary volumetric (mass) crystal size distributions of struvite produced at pH 8.5 (τ 900 and 3600 s) and 10 (τ 3600 s). With the increase in pH dominant crystal size (L_d, corresponding to peak in differential size distribution) shifts towards smaller crystal sizes: 66.9 μm (pH 8.5, τ 3600 s) → 38.0 μm (pH 10, τ 3600 s). Number and size of the largest product crystals decrease, as well. The largest size of struvite crystals produced at pH 8.5 is 220 μm (Fig. 3b), while at pH 10 – only 170 μm (Fig. 3c). Simultaneously fraction of the smallest crystals increases. In struvite population produced at pH 8.5 crystal fraction of sizes below 5 μm was 3.8%, while at pH 10 it raised up to 7.6%, thus 2-time increase is observed. In effect mean crystal size L_m decreased significantly from 72.8 to 40.1 μm (see tests No. 7 and 9 in Table 1). Elongation of mean residence time of suspension in a crystallizer from 900 to 3600 s produced, that dominant size L_d of struvite crystals shifted towards larger values: from 28.7 μm (τ 900 s, Fig. 3a) up to 64.9 μm (τ 3600 s, Fig. 3b). Size of the largest crystals in respect to whole population reached 155 and 220 μm, appropriately. Fines fraction in a product decreased from 10.1% (τ

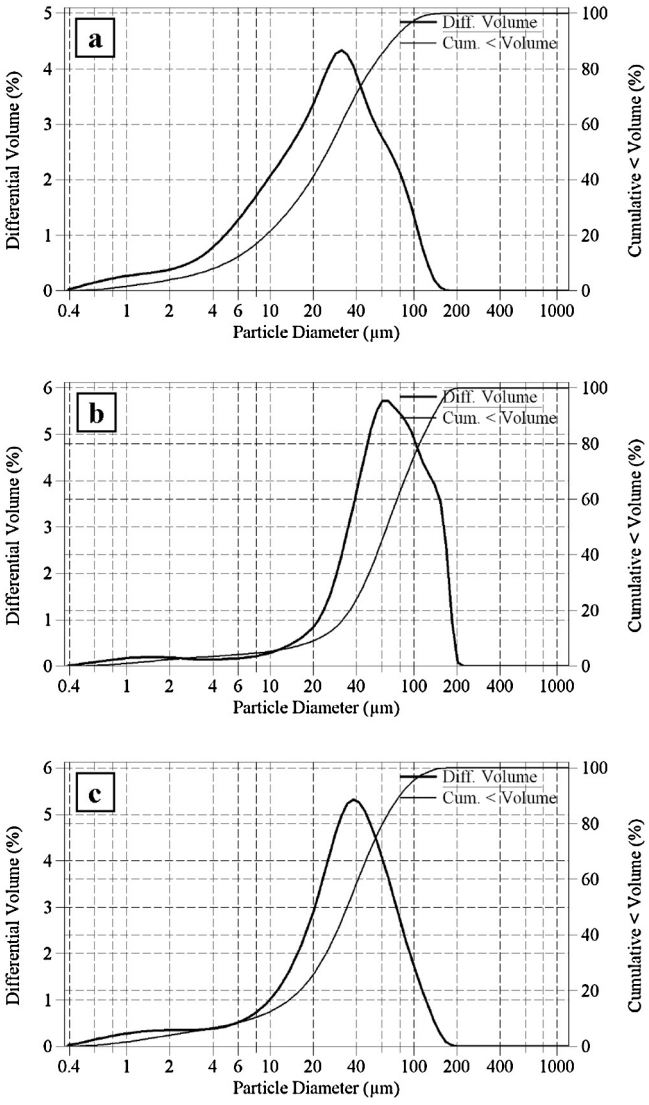

Fig. 3 – Exemplary differential (left scale) and cumulative (right scale) volumetric (mass) size distributions of struvite crystals produced in a continuous DT MSMPR crystallizer. Process parameters: (a) pH 8.5, τ 900 s, (b) pH 8.5, τ 3600 s, and (c) pH 10, τ 3600 s (tests No. 1, 7 and 9 in Table 1).

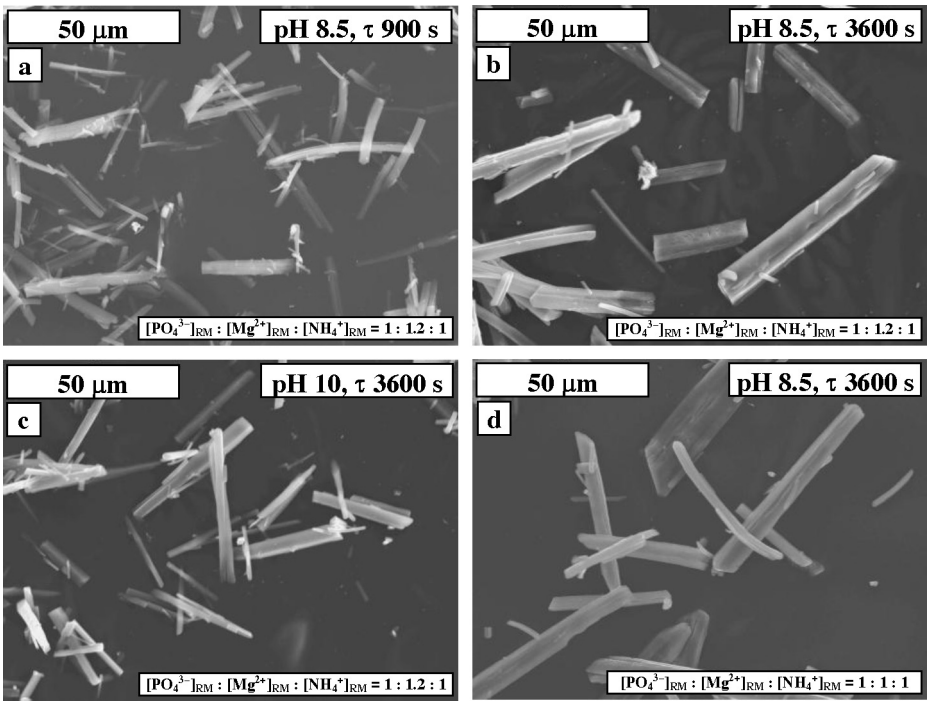

Fig. 4 – Scanning electron microscope images of struvite crystals produced in a continuous DT MSMPR crystallizer. Concentration of phosphate(V) ions in a feed $[PO_4^{3-}]_{RM}$ 0.20 wt%. Mean size of product crystals L_m: (a) 32.9 μm (pH 8.5, τ 900 s), (b) 72.8 μm (pH 8.5, τ 3600 s), (c) 40.1 μm (pH 10, τ 3600 s) – see Table 1 and Fig. 3, and (d) 110.2 μm (pH 8.5, τ 3600 s; Kozik and Matynia, 2012). Scanning electron microscope JEOL JSM 5800LV.

900 s) to 3.8% (τ 3600 s). From the data comparison (Fig. 3a and b) it results, that 4-time elongation of mean residence time influenced CSD of struvite advantageously. Number of the smallest crystals (of $L < 5$ μm) decreased (2.6×), size of the largest crystals increased by 65 μm, statistical CSD parameters (L_m, L_{50}, L_d) enlarged by more than 2-time and population homogeneity increased visibly (CV decreased by 22.5%) (see tests No. 1 and 7, Table 1).

3.2. *Crystal shape*

In Fig. 4a–c there are presented scanning electron microscope images of struvite crystals which size distributions are demonstrated in Fig. 3. In Fig. 4d – for comparison – there were shown images of struvite crystals produced under stoichiometric conditions in the same DT MSMPR crystallizer fed with solution of identical concentration 0.20 wt% PO_4^{3-} (Kozik and Matynia, 2012). Diverse sizes of struvite particles are clearly observable. The largest crystals corresponded to low pH and elongated mean residence time of suspension in a crystallizer. Mean size of these crystals L_m was ca. 73 μm, dominant size L_d ca. 67 μm and CV was lower than 60% (test No. 7 in Table 1, Fig. 4b). Under stoichiometric conditions crystal characteristic sizes were: L_m ca. 110 μm, L_d ca. 140 μm and CV 58% (Fig. 4d) (Kozik and Matynia, 2012). Crystal length L_a to their width L_b ratio was 7.7 in average (Fig. 4b) (under stoichiometric conditions: 7.5; Fig. 4d). The L_a/L_b values were calculated from planimetric measurements covering 50 crystals randomly selected from three different scanning electron microscope images of the same product sample. From the measurements it results, that for all product crystals L_a/L_b varied within the 5.3–7.7 range. The shortest and the thinnest crystals were produced at high pH (L_a/L_b 5.8; Fig. 4c) and short mean residence time (L_a/L_b 6.8; Fig. 4a). Reduction of pH and elongation of mean residence time resulted in significantly longer and thicker struvite crystals. Despite L_b raise, L_a/L_b was 7.7 (Fig. 4b). Struvite crystals produced from synthetic wastewater (Table 1) differ, however, in shape from the crystals produced from real wastewaters. This shape is significantly affected by impurities (Hutnik et al., 2011a). Struvite produced from wastewater from phosphorus mineral fertilizers industry demonstrated L_a/L_b ratio varying from 3.4 to 4.9 (Hutnik et al., 2013). Its crystals were shorter and simultaneously thicker. Their surface was partly occupied by co-precipitating and co-crystallizing solid impurities. It generated also large tensions within these crystal structures (cracks, trough-like crystal forms, etc.). From the analysis of scanning microscope images of the products (Fig. 4a–c) it also results, that geometrical shape of struvite crystals was diverse. Prismatic, needle-like particles and even tubular crystals of deformed, irregular edges were observed. Volume shape factor k_v of these solids varied typically from 0.010 to 0.040, for L_a:L_b:L_c 10:1:1 and 5:1:1, appropriately (Mersmann, 1995). If the particles are elongated or needle-shaped, their volume may be calculated on the assumption that they are cylindrical (Mullin, 1993). Calculated under this assumption mean k_v values were: 0.017 (pH 8.5, τ 900 s, L_a/L_b 6.8; Fig. 4a), 0.013 (pH 8.5, τ 3600 s, L_a/L_b 7.7; Fig. 4b) and 0.023 (pH 10, τ 3600 s, L_a/L_b 5.8; Fig. 4c). Agglomeration effects were not significant, while attrition and breakage of crystals during their intensive mixing and circulation in a crystallizer can be regarded moderate. Single broken crystals, surface damages, partly destructed corners were observed, however number of such crystals was not large. Generally it speaks advantageously about process conditions established in a DT MSMPR crystallizer for the continuous nucleation and struvite crystals growth.

3.3. *Chemical composition*

It was concluded, that concentration of phosphate(V) ions in a postprocessed mother liquor $[PO_4^{3-}]_{ML}$ varied from 92 mg/kg (pH 8.5, τ 900 s) to 9 mg/kg (pH 10, τ 3600 s) (Table 1). These

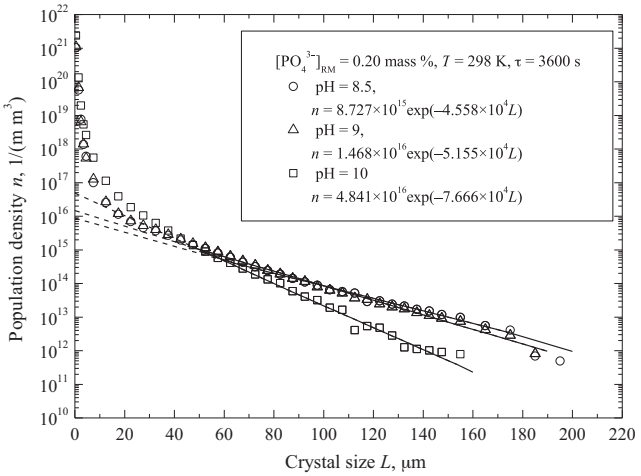

Fig. 5 – Influence of continuous struvite reaction crystallization environment's pH on population density distribution of product crystals: the points – experimental data, solid lines – the $n(L)$ values calculated with Eq. (2) valid for crystal fraction $L > 50\,\mu m$ (tests No. 7, 8 and 9 in Table 2).

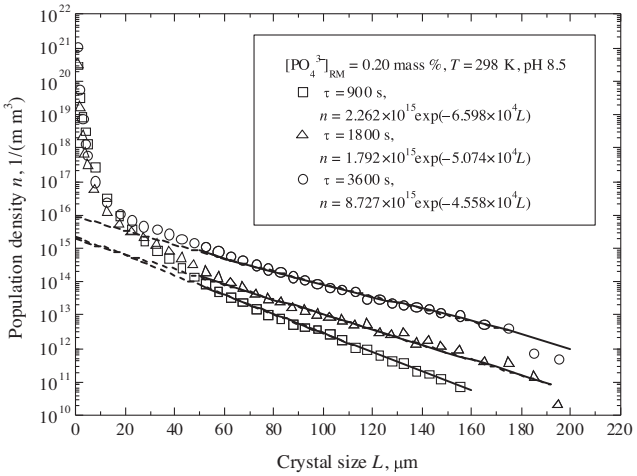

Fig. 6 – Influence of mean residence time of suspension in a crystallizer τ on population density distribution of product crystals: the points – experimental data, solid lines – the $n(L)$ values calculated with Eq. (2) valid for crystal fraction $L > 50\,\mu m$ (tests No. 1, 4 and 7 in Table 2).

residual concentrations decreased systematically both with pH rise and with elongation of mean residence time τ of struvite crystal suspension in a crystallizer. Moreover, from Table 1 it results, that even 10-time reduction of residual $[PO_4^{3-}]_{ML}$ concentration can be achieved. It is attributed to mentioned earlier decreasing of struvite solubility with the increase in pH of the reaction mixture and with longer contact time of crystals with the supersaturated solution (more thorough discharge of the generated supersaturation). The $[PO_4^{3-}]_{ML}$ values in the discussed tests can be considered small, thus effectiveness of phosphate(V) ions removal from the feed (of $[PO_4^{3-}]_{RM}$ 0.20 wt%) as a fully satisfactory: from 95.4% (pH 8.5, τ 900 s) up to 99.5% (pH 10, τ 3600 s).

Excess of magnesium ions in respect to phosphate(V) and ammonium ions influenced process yield advantageously. Residual concentration of phosphate(V) ions in a postprocessed mother solution was significantly smaller than in the comparable process driven under stoichiometric conditions (Le Corre et al., 2007b). For the tests carried out under stoichiometric conditions (Kozik and Matynia, 2012) corresponding $[PO_4^{3-}]_{ML}$ values were 220 and 95 mg/kg for pH 8.5 and τ 900 s, as well as for pH 10 and τ 3600 s, respectively. These values are from ca. 2- to 10-time higher compared to the ones determined analytically in a postprocessed mother liquor in presence of magnesium ions excess (Table 1).

3.4. *Nucleation and crystal growth kinetics*

In Fig. 5 there are presented the experimental population density distributions of struvite crystals produced at pH 8.5, 9 and 10, for mean residence time of suspension in a crystallizer 3600 s (see Figs. 3b,c and 4b,c for pH 8.5 (b) and 10 (c)). Influence of mean residence time τ 900, 1800 and 3600 s (pH 8.5) on population density distribution of struvite crystals is presented in Fig. 6 (see Figs. 3a,b and 4a,b for τ 900 (a) and 3600 s (b)). From these distribution courses, presented in $\ln n - L$ coordinates, it results, that for struvite particles of size $L > 50\,\mu m$ these dependencies can be, with satisfactory precision, approximated with linear function (→SIG kinetic model). From Eq. (2) one can calculate linear crystal growth rate G, and from Eq. (3) their nucleation rate B. Estimated parameter values of population density distributions for struvite crystals of size $L > 50\,\mu m$ (detailed forms of Eq. (2)) and calculated on this basis G and B values are presented in Table 2.

From the analysis of experimental data (Figs. 3 and 4) and $\ln n(L)$ courses (Figs. 5 and 6) it results, that SIG MSMPR model assumptions are not strictly fulfilled. Nonlinear course of population density distributions for crystals of size smaller than 50 μm (in $\ln n - L$ coordinates, Figs. 5 and 6) suggests more complex kinetics than it results from the assumed SIG kinetic model (Randolph and Larson, 1988; Mullin, 1993). Concave to top in $\ln n(L)$ course for $L < 50\,\mu m$ suggests, that crystal linear growth rate depends on its size (*Size Dependent Growth*, SDG) (Koralewska et al., 2009), each crystal grows with intrinsic, individual rate (*Growth Rate Dispersion*, GRD) (Harrison et al., 2011) or crystal attrition occurs (Mersmann, 1995). Thus kinetic parameter values of the process determined with this method should be regarded as a rough approximation only. It especially concerns nucleation rate B values calculated from Eq. (3), with the use of strongly devaluated nuclei population density n_0 values ($n(L)$ for $L = 0$). As it results from Figs. 5 and 6, the possible Δn_0 differences between n_0 values predicted by extrapolation with the use of linear kinetic SIG model and their real values reached even 10^5. Calculated with SIG kinetic model B values are thus practically useful only for relative, conventional comparison of the tested parameters influence on the process course and its final results.

Analyzing the kinetic data presented in Table 2 one can notice regular decreasing trend of crystals linear growth rate G with the raise of pH. For example, increase in crystallizer environment's pH from 8.5 to 10 for τ 3600 s produced decrease of G from 6.09×10^{-9} to 3.62×10^{-9} m/s. It is a significant decrease of G (by ca. 40%). It is accompanied by increase in the values of nuclei population density n_0 (from 8.7×10^{15} to 4.8×10^{16} 1/(m m^3); by 5.5×), thus in nucleation rate B (from 5.3×10^7 to 1.7×10^8 1/(m^3 s); by 3.2×). In result final mean crystal size L_m decreased (72.8 → 40.1 μm).

Generally higher values of crystal growth rate are observed for the shortest mean residence times of suspension in a crystallizer (Mullin, 1993). It is in conformity with observations concerning classical continuous mass crystallization processes. Mean G values (within pH 8.5–10) are: 1.42×10^{-8},

8.49×10^{-9} and 5.03×10^{-9} m/s for τ 900, 1800 and 3600 s, respectively. These values decrease in proportion 2.8:1.7:1. Nucleation rate B, similarly to linear crystal growth rate G, decreases with the elongation of mean residence time τ of suspension in a crystallizer. Elongation of τ corresponds to decrease of working supersaturation in a process system (Mullin, 1993). Exception from this rule for τ 3600 s was, however, reported (see Table 2). For example, at pH 8.5 the B values are: 3.9×10^{7}, 2.0×10^{7} and 5.3×10^{7} 1/(m^3 s) for τ 900, 1800 and 3600 s, respectively. For the longest mean residence time nucleation rate enlarged. Crystal attrition and breakage were more intense for 2-time longer (compared to τ 1800 s) residence (thus vigorous mixing) time in a crystallizer. Despite higher nucleation rate, product of larger particle sizes was obtained (L_m 32.9 μm < 51.7 μm < 72.8 μm for τ 900, 1800 and 3600 s, respectively, Table 1). Lower values of linear growth rate and higher values of nucleation rate (for τ 3600 s) are compensated, with excess, by longer contact time of crystals with supersaturated mother liquor. It influences solid phase growth and resulting CSD of struvite suspension advantageously. More convenient conditions of mass transfer between liquid and solid phase establish, additionally providing more stable crystal growth. In a process system characterized by relatively long mean residence time, higher quality struvite product is manufactured, of larger crystal sizes (L_m 32.9 → 72.8 μm, pH 8.5) and of higher homogeneity (CV 82.3 → 59.8%, pH 8.5).

In Table 2, for comparison, other struvite linear crystal growth rates and nucleation rates were also provided. These correspond to continuous DT MSMPR crystallizer fed with synthetic wastewater ($[PO_4^{3-}]_{RM}$ 0.20 wt%, stoichiometric conditions; Kozik and Matynia, 2012) and to phosphorus fertilizers industry wastewater ($[PO_4^{3-}]_{RM}$ 0.445 wt%, magnesium ions excess; Hutnik et al., 2013). In synthetic wastewater under stoichiometric conditions linear crystal growth rates of struvite were higher (by ca. 27% on average), while nucleation rates were generally lower (by ca. 38% on average). Contrary, in a real industrial wastewater, linear growth rates were lower from ca. 13 to ca. 21%, while nucleation rates were even 7-time higher (No. 2, Table 2). From the comparison it results, that the reason of such large differences in kinetic parameter values was magnesium ions excess in relation to concentration of phosphate(V) ions in a feed (synthetic wastewater) and presence of impurities in industrial wastewater. Lower linear growth rate and higher nucleation rate cause in result deteriorate of product quality. For example, under pH 9 and τ 3600 s: L_m 72.5 μm, CV 59.3% (Kozik and Matynia, 2012), L_m 48.5 μm, CV 64.6% – Table 1, L_m 36.8 μm, CV 74.7% (Hutnik et al., 2013).

Harrison et al. (2011) determined so called initial growth rates of struvite in batch crystallization conditions. Pilot scale studies on wastewater stream at local abattoir demonstrated, that these rates varied from 0.45 to 0.8 μm/min (7.5×10^{-9} to 1.3×10^{-8} m/s) at pH 8.5. In a struvite continuous reaction crystallization process G varied from 6.09×10^{-9} to 1.68×10^{-8} m/s (pH 8.5, synthetic wastewater, Table 2) and from 4.27×10^{-9} to 1.43×10^{-8} m/s (pH 9, industrial wastewater (Hutnik et al., 2013)). From the comparison good conformity of the results can be observed, in spite of essential differences in both crystallization process regimes: batch and continuous.

4. Conclusions

From the continuous DT MSMPR type crystallizer struvite crystals of mean size L_m from 18.8 to 72.8 μm were removed. It was identified experimentally, that increase in pH (from 8.5 to 10) of struvite reaction crystallization environment produced decrease of mean crystal size by ca. 44% on average. However, elongation of mean residence time of suspension in a crystallizer from 900 to 3600 s resulted in a significant raise of this characteristic size (even more than 2-time). Struvite crystal products of diverse size-homogeneity (CV 59.8–87.4%) were removed from the crystallizer. It is net effect of a complex influence of pH and mean residence time of suspension, contributed by attrition and breakage within crystals on the resulting supersaturation level self-establishing in a mother liquor.

For the estimation of process kinetic parameter values the simplest SIG kinetic model valid for ideal MSMPR crystallizer was used. It was concluded, that linear growth rate of struvite crystals varied within the 3.62×10^{-9} to 1.68×10^{-8} m/s range, whereas nucleation rate within the 2.0×10^{7}–3.1×10^{8} 1/(s m^3) limits. With the pH raise nucleation rate increased, while crystal linear growth rate decreased. Decrease of G with the elongation of mean residence time of suspension was accompanied by advantageous raise of mean size L_m of struvite product crystals. Lower values of linear growth rate were thus compensated, with excess, by longer contact time of crystals with the supersaturated mother solution. In process conditions characterized by relatively long mean residence time of suspension in a crystallizer, higher quality struvite product is manufactured. However, the unit productivity is small, thus economic effectiveness of a whole production plant is lower.

Magnesium ions excess in a process system influenced the continuous struvite reaction crystallization process yield advantageously, however significantly smaller product crystals were observed. Concentration of phosphate(V) ions in a postprocessed mother liquor decreased from inlet 0.20 wt% to 0.9×10^{-3} – 9.2×10^{-3} wt% (9–92 mg/kg) depending on combination of pH and mean residence time of suspension in a crystallizer. It can be regarded as a very good effectiveness of their recycling process from the inlet solution.

Acknowledgements

This work was supported by the National Science Centre of Poland under Grant No. NN209 1174 37 (2009–2012).

References

Ali, Md.I., Schneider, P.A., 2006. A fed-batch design approach of struvite system in controlled supersaturation. Chem. Eng. Sci. 61, 3951–3961.

Bhuiyan, M.I.H., Mavinic, D.S., Beckie, R.D., 2007. A solubility and thermodynamic study of struvite. Environ. Technol. 28, 1015–1026.

Bhuiyan, M.I.H., Mavinic, D.S., Koch, F.A., 2008. Phosphorus recovery from wastewater through struvite formation in fluidized bed reactors: a sustainable approach. Water Sci. Technol. 57, 175–181.

Bouropoulos, N.C., Koutsoukos, P.G., 2000. Spontaneous precipitation of struvite from aqueous solutions. J. Cryst. Growth 213, 381–388.

de-Bashan, L.E., Bashan, Y., 2004. Recent advances in removing phosphorus from wastewater and its future use as fertilizer. Water Res. 38, 4222–4246.

Doyle, J.D., Parsons, S.A., 2002. Struvite formation, control and recovery. Water Res. 36, 3925–3940.

Doyle, J.D., Parsons, S.A., 2004. Struvite scale formation and control. Water Sci. Technol. 49, 177–182.

Franke, J., Mersmann, A., 1995. The influence of the operational conditions on the precipitation process. Chem. Eng. Sci. 50, 1737–1753.

Gadekar, S., Pullammanappallil, P., 2010. Validation and applications of a chemical equilibrium model for struvite precipitation. Environ. Monit. Assess. 15, 201–209.

Harrison, M.L., Johns, M.R., White, E.T., Mehta, C.M., 2011. Growth rate kinetics for struvite crystallization. Chem. Eng. Trans. 25, 309–314.

Hutnik, N., Piotrowski, K., Gluzinska, J., Matynia, A., 2011a. Effect of selected inorganic impurities present in real phosphate(V) solutions on the quality of struvite crystals produced in continuous reaction crystallization process. Prog. Environ. Sci. Technol. 3, 559–566.

Hutnik, N., Piotrowski, K., Wierzbowska, B., Matynia, A., 2011b. Continuous reaction crystallization of struvite from phosphate(V) solutions containing calcium ions. Cryst. Res. Technol. 46, 443–449.

Hutnik, N., Kozik, A., Mazienczuk, A., Piotrowski, K., Wierzbowska, B., Matynia, A., 2013. Phosphates(V) recovery from phosphorus mineral fertilizers industry wastewater by continuous struvite reaction crystallization process. Water Res. 47, 3635–3643.

Karabegovic, L., Uldal, M., Werker, A., Morgan-Sagastume, F., 2013. Phosphorus recovery potential from a waste stream with high organic and nutrient contents via struvite precipitation. Environ. Technol. 34, 871–883.

Kofina, A.N., Koutsoukos, P.G., 2005. Spontaneous precipitation of struvite from synthetic wastewater solutions. Cryst. Growth Des. 5, 489–496.

Koralewska, J., Piotrowski, K., Wierzbowska, B., Matynia, A., 2009. Kinetics of reaction crystallization of struvite in the continuous draft tube magma type crystallizers – influence of different internal hydrodynamics. Chin. J. Chem. Eng. 17, 330–339.

Kozik, A., Matynia, A., 2012. Continuous reaction crystallization of struvite under stoichiometric conditions. Przem. Chem. 91, 823–827.

Kozik, A., Hutnik, N., Piotrowski, K., Mazienczuk, A., Matynia, A., 2013. Precipitation and crystallization of struvite from synthetic wastewater under stoichiometric conditions. Adv. Chem. Eng. Sci. 3, 20–26.

Latifian, M., Liu, J., Mattiasson, B., 2012. Struvite-based fertilizer and its physical and chemical properties. Environ. Technol. 33, 2691–2697.

Le Corre, K.S., Valsami-Jones, E., Hobbs, P., Parsons, S.A., 2005. Impact of calcium on struvite crystal size, shape and purity. J. Cryst. Growth 283, 514–522.

Le Corre, K.S., Valsami-Jones, E., Hobbs, P., Parsons, S.A., 2007a. Impact of reactor operation on success of struvite precipitation from synthetic liquors. Environ. Technol. 28, 1245–1256.

Le Corre, K.S., Valsami-Jones, E., Hobbs, P., Parsons, S.A., 2007b. Kinetics of struvite precipitation: effect of magnesium dose on induction times and precipitation rates. Environ. Technol. 28, 1317–1324.

Le Corre, K.S., Valsami-Jones, E., Hobbs, P., Parsons, S.A., 2009. Phosphorus recovery from wastewater by struvite crystallization: a review. Crit. Rev. Environ Sci. Technol. 39, 433–477.

Marti, N., Pastor, L., Bouzas, A., Ferrer, J., Seco, A., 2010. Phosphorus recovery by struvite crystallization in WWTPs: influence of the sludge treatment line operation. Water Res. 44, 2371–2379.

Matynia, A., Koralewska, J., Piotrowski, K., Wierzbowska, B., 2006. The influence of the process parameters on the struvite continuous crystallization kinetics. Chem. Eng. Commun. 193, 160–176.

Mazienczuk, A., Hutnik, N., Piotrowski, K., Wierzbowska, B., Matynia, A., 2012. Continuous crystallizers with jet pump driven by recirculated mother solution in production of struvite. Przem. Chem. 91, 890–895.

Mersmann, A. (Ed.), 1995. Crystallization Technology Handbook. M. Dekker, Inc., New York.

Mullin, J.W., 1993. Crystallization. Butterworth-Heinemann, Oxford.

Ohlinger, K.N., Young, T.M., Schroeder, E.D., 1998. Predicting struvite formation in digestion. Water Res. 32, 3607–3614.

Parsons, S.A., 2001. Recent scientific and technical developments: struvite precipitation. CEEP Scope Newslett. 41, 15–22.

Penicot, P., Muhr, H., Plesari, E., Villermaux, J., 1998. Influence of the internal crystallizer geometry and the operational conditions on the solid product quality. Chem. Eng. Technol. 21, 507–513.

Randolph, A.D., Larson, M.A., 1988. Theory of Particulate Processes: Analysis and Techniques of Continuous Crystallization. Academia Press, New York.

Snoeyink, V.L., Jenkins, D., 1980. Water Chemistry. Wiley, New York.

Söhnel, O., Garside, J., 1992. Precipitation: Basic Principles and Industrial Applications. Butterworths-Heinemann, Oxford.